

Title: The canonical semantic network supports residual language function in chronic post-stroke aphasia

Authors: Joseph C. Griffis¹, Rodolphe Nenert², Jane B. Allendorfer², Jennifer Vannest³, Scott Holland³, Aimee Dietz⁴, Jerzy P. Szaflarski²

Institutional Affiliations: University of Alabama at Birmingham Department of Psychology¹, University of Alabama at Birmingham Department of Neurology², Cincinnati Children's Hospital Medical Center, Cincinnati, OH³, University of Cincinnati Academic Health Center, Cincinnati, OH⁴

Abstract

Current theories of language recovery after stroke are limited by a reliance on small studies. Here, we aimed to test predictions of current theory and resolve inconsistencies regarding right hemispheric contributions to long-term recovery. We first defined the canonical semantic network in 43 healthy controls. Then, in a group of 43 patients with chronic post-stroke aphasia, we tested whether activity in this network predicted performance on measures of semantic comprehension, naming, and fluency while controlling for lesion volume effects. Canonical network activation accounted for 22-33% of the variance in language test scores. Whole-brain analyses corroborated these findings, and revealed a core set of regions showing positive relationships to all language measures. We next evaluated the relationship between activation magnitudes in left and right hemispheric portions of the network, and how right hemispheric activation related to the extent of left hemispheric damage. Activation magnitudes in the each hemispheric network were strongly correlated, but four right frontal regions showed heightened activity in patients with large lesions. Activity in two of these regions (inferior frontal gyrus pars opercularis and supplementary motor area) was associated with better language abilities in patients with larger lesions, but poorer language abilities in patients with smaller lesions. Our results indicate that bilateral language networks support language processing after stroke, and that right hemispheric activations related to extensive left hemisphere damage occur outside of the canonical semantic network and differentially contribute to in their relationship to behavior depending on the extent of left hemispheric damage.

Introduction

Functional neuroimaging of language recovery after stroke

Aphasia commonly occurs in patients with strokes affecting the left middle cerebral artery (LMCA) territory, and is of the most debilitating consequences of stroke since language impairments affect nearly every aspect of daily life [Maas et al., 2012]. Language recovery after LMCA stroke is variable, with many survivors experiencing chronic deficits [Charidimou et al., 2014; Lazar et al., 2008; Pedersen, 1995]. Current theories of aphasia recovery are based primarily on evidence obtained from functional neuroimaging studies [Heiss and Thiel, 2006; Saur and Hartwigsen, 2012; Turkeltaub et al., 2011]. During early recovery, patients have been observed to show up-regulation of right hemispheric responses to language tasks that are thought to reflect a transient compensatory mechanism triggered by the acute disruption of left hemispheric function [Hartwigsen et al., 2013; Saur et al., 2006; Thiel et al., 2006]. In later stages of recovery, the gradual reinstatement of left hemispheric capacity for language processing is thought to decrease the need for right hemispheric compensation, resulting in a return of relatively balanced hemispheric activation patterns [Heiss and Thiel, 2006; Saur et al., 2006; Saur and Hartwigsen, 2012; Turkeltaub et al., 2011]. Thus, the general principle inferred from functional neuroimaging studies of language recovery after stroke might be summarized as follows: good long-term language outcomes depend primarily on the preservation or restoration of close-to-normal function in canonical brain language networks.

While there is consistent support in the literature for a primary role of the canonical left hemispheric language networks in enabling language recovery after stroke, the role of the right hemisphere is less clear. For example, there is evidence that activation of right inferior frontal [Griffis et al., 2016a; Rosen et al., 2000; Winhuisen et al., 2005; Winhuisen et al., 2007] and right superior temporal [Karbe et al., 1998; Szaflarski et al., 2013] areas during language tasks may negatively impact performance, although there is also evidence that activation of right inferior frontal [Mattioli et al., 2014; van Oers et al., 2010; Raboyeau et al., 2008; Saur et al., 2006] and right anterior superior temporal [Crinion and Price, 2005] regions may be beneficial for recovery. One

explanation for such seemingly discrepant relationships is that when the left hemisphere is not sufficiently preserved, the initial reliance on right hemispheric language network homologues persists beyond early recovery, and the lack of left hemispheric involvement leads to poorer recovery relative to when left hemispheric function is successfully restored [Heiss et al., 1999; Heiss and Thiel, 2006; Karbe et al., 1998; Szaflarski et al., 2013; Turkeltaub et al., 2011]. In this case, the direction of the observed relationship between right hemispheric activations and language functions might depend on the sample, since right hemispheric activation might show a positive relationship to language abilities in a sample that primarily consists of severely impaired patients, and a negative relationship in a sample that includes patients with all degrees of impairments [Saur and Hartwigsen, 2012].

Sample sizes in functional neuroimaging studies of aphasia recovery

A limitation shared by many of the studies that form the foundation for current theory is the use of small patient samples [Saur and Hartwigsen, 2012], which may contribute to discrepancies in the literature. To illustrate the prevalence of small sample sizes in functional neuroimaging studies of post-stroke aphasia, we identified 82 such studies published since 1995 using Google Scholar with search terms such as “aphasia fmri”, “aphasia pet”, “aphasia neuroimaging”, “aphasia recovery”, and “language recovery after stroke”. Across all 82 studies, the average patient sample size was only about 10 patients (mean = 9.76, SD = 7.05), and the single largest sample was 30 patients (Figure 1 and Supplemental Table 1). The dependence of current theory on results obtained from small studies is problematic for several reasons. For example, it has previously been noted in the context of neuroimaging studies that power to detect between-subject effects is reduced in small samples [Yarkoni, 2009]. This makes smaller studies less likely to detect relationships based on individual differences – and these relationships are often of primary interest in neuroimaging studies of language recovery after stroke. In addition to reducing power, small sample sizes lead to inflated estimates of effect size. Indeed, correlation estimates are substantially inflated for studies with less than 30 patients -- for a relationship with a population r of 0.3, the average observed sample r in samples of 20 patients is expected to be around 0.73 [Yarkoni, 2009]. This

suggests that even for samples twice the average size of samples studied in the literature, correlation estimates can be expected to be inflated by over twice their true values. Based on these observations, a majority of previous functional MRI studies of aphasia recovery are likely to have (1) failed to detect real brain-behavior relationships, and (2) reported inflated estimates of detected relationships. Since the dependence of the field on small studies has the potential to produce an incomplete and distorted theory of recovery, we contend that it is necessary to test the predictions of current theory in larger patient samples.

Statistical control for lesion volume in functional neuroimaging of aphasia recovery

A second limitation shared by most functional neuroimaging studies of language recovery after stroke is a lack of statistical control for lesion volume effects on imaging-behavior relationships. This is somewhat surprising given that the use of statistical controls to reduce confounds related to lesion volume effects is relatively common in lesion-symptom mapping research [Rorden and Karnath, 2004; Schwartz et al., 2009; Yongsheng et al., 2014]. The logic behind using statistical controls to account for lesion volume effects is that since (1) larger lesions are often associated with more severe impairments [Allendorfer et al., 2012; Butler et al., 2014; Cheng et al., 2014; Karnath et al., 2004; Kümmerer et al., 2013; Meltzer et al., 2013; van Oers et al., 2010; Rorden and Karnath, 2004; Szaflarski et al., 2013; Yarnell et al., 1976], and (2) larger lesions have a higher probability of including both task-relevant and task-irrelevant voxels [Karnath et al., 2004; Rorden and Karnath, 2004; Schwartz et al., 2009; Yongsheng et al., 2014], lesion volume effects have the potential to introduce bias into measurements of lesion-behavior relationships at voxels that are primarily damaged in patients with large lesions [Karnath et al., 2004; Yongsheng et al., 2014]. In functional neuroimaging, the probability that a voxel is active during task performance depends on the probability that the tissue at that voxel is spared, and the probability that the tissue at a given voxel in the left hemisphere is spared depends on the size of the lesion. Therefore, the potential for lesion volume confounds is logically extendable to relationships between functional neuroimaging activation and behavior.

Study aims and hypotheses

In the current study, we first tested what we consider to be the primary prediction of current models of language recovery after stroke: that successful long-term recovery depends on the preservation/restoration of language task-driven activation in semantic language networks. To test this prediction, we first defined the canonical semantic network activated by semantic decisions in healthy controls. We then assessed relationships between task-evoked activity in this network and measures of language function using a comparatively large sample of LMCA stroke patients with chronic aphasia. To reduce the potential for bias and to assess the stability of our results, we evaluated this relationship both with and without statistical control for lesion volume effects. Additionally, we tested the explanation that right hemispheric activation in chronic patients reflects compensation driven by a reduced capacity of the left hemisphere to perform language-related processing. Under this explanation, we expected activation in right hemispheric portions of the semantic network to be negatively related to activation in left hemispheric portions of the network, and positively related to lesion volume. Finally, because we are not aware of any studies that have directly measured the effect of left hemispheric lesion volume on regional activation in the right hemisphere, we characterized regions in the right hemisphere where task-driven responses correlated with total lesion volume and assessed whether activity in these regions might reflect beneficial compensation in patients with larger lesions.

Materials and Methods

Participants

All study procedures were approved by the Institutional Review Boards of the participating institutions and were performed in accordance with Declaration of Helsinki ethics principles and principles of informed consent. For the current study, we used functional MRI data collected from 43 chronic post-stroke aphasia patients and 43 healthy controls. Imaging and behavioral data for the post-stroke aphasia patients were collected for several studies performed by our laboratory. Prior to inclusion, all

participants were screened to exclude individuals that had diagnoses of degenerative/metabolic disorders, had severe depression or other psychiatric disorders, were pregnant, were not fluent in English, or had any contraindication to MRI/fMRI. Patients were included in the current study if they had a single left hemispheric stroke resulting in aphasia at least 1 year prior to data collection. Data for the control participants were selected from a database of 150 healthy individuals collected for several studies performed by our laboratory, and were selected based on age group (19-29, 30-39, 40-49, 50-59, 60+), handedness as determined by the Edinburgh Handedness Inventory [Oldfield, 1971], and sex to minimize differences in demographics with respect to the patient group. Participant demographics are shown in Table 1.

Language measures

Prior to MRI scanning, all participants were administered a battery of neuropsychological language assessments. All participants performed the Boston Naming Test (BNT) [Kaplan et al., 2001], Semantic Fluency Test (SFT) [Kozora and Cullum, 1995], and Controlled Oral Word Association Test (COWAT) [Lezak et al., 1995]. The BNT requires patients to name a series of black and white line drawings that contain both animate and inanimate items that vary in frequency of use (e.g. bed vs. abacus), and the number of correctly named pictures serves as a measure of naming ability. The SFT requires patients to generate as many words as they can think of that fit a given category prompt (e.g. animals) within a one-minute time limit, and the number of words generated serves as a measure of category fluency. The COWAT requires patients to generate as many words as they can think of that begin with a particular letter (e.g. A) within a one-minute time limit, and the number of words generated serves as a measure of phonemic fluency. Performance scores for the COWAT and SFT were very strongly correlated across patients ($r=0.92$), so they were averaged together to define a single combined measure of verbal fluency. Performance scores for the verbal fluency measure were correlated, albeit less strongly, with performance scores for the BNT ($r=0.76$).

Neuroimaging data collection

MRI Data were collected at the University of Alabama at Birmingham using a 3T head-only Siemens Magnetom Allegra scanner located in the Civitan International Research Center Functional Imaging Laboratory. These data consisted of 3D high-resolution T1-weighted anatomical scans (TR/TE = 2.3 s/2.17 ms, FOV = 25.6×25.6×19.2 cm, matrix = 256×256, flip angle = 9 degrees, slice thickness = 1mm), and two T2*-weighted gradient-echo EPI pulse functional scans (TR/TE = 2.0 s/38.0 ms, FOV = 24.0×13.6×24.0, matrix = 64×64, flip angle = 70 degrees, slice thickness = 4 mm, 165 volumes per scan). MRI data were also collected at the Cincinnati Children's Hospital Medical Center on a 3T research-dedicated Phillips MRI system located in the Imaging Research Center. These data consisted of 3D high-resolution T1-weighted anatomical scans (TR/TE = 8.1 s/2.17 ms, FOV = 25.0×21.0×18.0 cm, matrix = 252×211, flip angle = 8 degrees, slice thickness = 1mm) and two T2*-weighted gradient-echo EPI pulse sequence functional scans (TR/TE = 2.0 s/38.0 ms, FOV = 24.0×13.6×24.0, matrix = 64×64, flip angle = 70 degrees, slice thickness = 4 mm, 165 volumes per scan).

Functional MRI scans were acquired while participants completed alternating 30 second blocks of a semantic decision/tone decision task. This task was chosen because it has been previously shown to result in robust activation in canonical areas involved in language processing [Binder et al., 1997], and has been used extensively to evaluate language network activation in healthy and diseased populations that include patients with chronic post-stroke aphasia [Eaton et al., 2008; Szaflarski et al., 2008; Szaflarski et al., 2011]. The active condition (semantic decision -- SD) was performed 5 times during each scan. During each block of the active condition, participants heard eight spoken English nouns designating different animals and made decisions based on whether or not the animals satisfied the following criteria: "native to the United States" and "commonly used by humans". If both criteria were satisfied, then the participants responded "1" by using their non-dominant hand to press a button. If both criteria were not satisfied, then the participants responded "2" by using their non-dominant hand to press a second button. The control condition was performed 6 times during each scan. During each block of the control condition (tone decision -- TD), participants heard eight brief sequences of four to seven 500- and 750-Hz tones. If the sequence contained two 750-Hz tones, then they pressed the button designated "1" with their non-dominant hand. Else, participants

pressed the button designated “2” with their non-dominant hand. Each scan lasted 7 minutes and 15 seconds. Prior to completing the task in the MRI scanner, all participants confirmed their understanding of the task by performing a mock run that included a sequence of five sets of tones followed by a sequence of five nouns designating different animals. In-scanner task data were not collected for 4 patients due to hardware issues, and they were excluded from analyses investigating relationships between fMRI activation and in-scanner performance.

Neuroimaging data processing

All MRI data were processed using Statistical Parametric Mapping (SPM) [Friston et al., 1995] version 12 running in MATLAB r2014b (The MathWorks, Natick MA, USA). Functional MRI scans were pre-processed using a standard pre-processing pipeline consisting of slice-time correction, realignment/reslicing, co-registration of the fMRI data to the corresponding anatomical scan, unified segmentation with optimized tissue priors for lesioned brains and normalization of the anatomical scan to MNI space [Ripollés et al., 2012; Seghier et al., 2008], normalization of the functional scan to MNI space using the transformation applied to the anatomical scan, and spatial smoothing using an 8mm full-width half maximum Gaussian kernel. This pipeline enables accurate template registration and normalization even for patients with structural abnormalities such as those observed in stroke patients [Ripollés et al., 2012]. To reduce the potential for motion-related artifacts, functional scans were motion-corrected by replacing volumes with >0.5 mm motion with an interpolated volume created from adjacent volumes [Mazaika et al., 2005]. Lesion probability maps were created for each patient using a voxel-based naïve Bayes classification algorithm that was developed by our laboratory and is implemented in the *lesion_gnb* toolbox for SPM12 [Griffis et al., 2016b]. While automated classification with this method compares favorably to manual lesion delineation for large and small lesions [Griffis et al., 2016b], we opted to manually threshold the resulting posterior probability maps to ensure that they precisely reflected the extent of the lesion. The resulting binary lesion masks were used to estimate lesion volume and lesion-ROI overlaps, and were used in all further lesion analyses. Lesion frequencies across all 43 patients are shown in Figure 2A.

For each participant, the pre-processed fMRI data were fit to a general linear model (GLM) where task blocks were modeled as boxcar regressors convolved with a canonical hemodynamic response function (HRF). In order to account for variability in the time-to-peak of the HRF, time and dispersion derivatives were included as basis functions [Meinzer et al., 2013]. Note that since data were collected using a blocked design, separate modeling of correct vs. incorrect trials was not possible. Linear contrast estimate maps were then computed to quantify the difference in activation magnitudes between the active and control conditions. These contrast maps were used for all further functional MRI analyses.

Statistical Analyses

Group differences on behavioral measures were assessed for descriptive purposes using two-tailed independent samples t-tests with degrees of freedom adjustment for unequal variances.

To identify regions that showed significant group-level activation for each group, the first-level contrast estimate maps from all individuals in each group were entered into separate second-level *t* contrasts quantifying the difference in peak HRF magnitude between the SD and TD conditions. Regional activation was considered significant if it survived a combined voxel-level intensity (*p*-value) threshold of 0.01 and a cluster-level extent threshold of $p < 0.05$ corrected ($k_{crit} = 99$ voxels) to control the whole-brain family-wise error rate (FWE) at 0.05 as determined by 1000 Monte Carlo simulations [Slotnick et al., 2003]. The thresholded map obtained for the control group was then binarized, creating a canonical semantic network region-of-interest (ROI) mask where statistically significant voxels had a value of 1 and all other voxels had a value of 0. For each patient, the mean contrast estimate across all voxels within this canonical semantic network ROI was then extracted from their first-level contrast estimate map, quantifying the average magnitude of the task-driven response in the canonical semantic network. These estimates were used in subsequent ROI correlation analyses. Group differences in activation within the canonical semantic network were assessed for descriptive purposes using an independent samples t-test with degrees of freedom adjustment for unequal variances. Lesion-ROI overlaps were calculated for each patient using the lesion masks

created during pre-processing. The correlation between total lesion volumes and lesion-ROI overlaps indicated that lesion-ROI overlap was a close linear transformation of lesion volume ($r=0.93$).

To assess the unique relationships between activity in the canonical network and language function in chronic patients, the mean contrast estimate quantifying activation within the HC-defined canonical semantic network was then entered as an independent variable in 3 separate partial correlation analyses. The dependent variables for each analysis were the performance scores for the in-scanner SD task (% correct responses) and performance scores for the out-of-scanner naming and fluency tasks. Each model included total lesion volume as a covariate to account for variance attributable to lesion volume effects. Analyses were repeated without lesion volume control. To fully characterize relationships between regional language task activation and performance on the in-scanner and out-of-scanner language tasks, three whole-brain multiple regressions (one for each language task) were performed that each included lesion volume as a covariate, and were also repeated without lesion volume control.

To test whether the magnitude of activation in right hemispheric portions of the canonical network was increased in patients with lower levels of activation in left hemispheric portions of the network, the canonical semantic network ROI mask was split into left and right hemispheric components. For each patient, the mean contrast estimate was then extracted from each hemispheric ROI as described above. Linear correlations were assessed between the mean contrast estimates obtained from each hemisphere with and without lesion volume control. To explicitly test for this effect in right hemispheric homologues of the left hemisphere network and control for differences in extent between left and right hemispheric portions of the canonical network, these analyses were also repeated using a right hemispheric ROI that was defined by simply mirroring the left-hemispheric ROI to the right hemisphere. Correlations were also assessed between left hemispheric and right hemispheric activation in controls. Differences in activation between left and right hemispheric networks were assessed with dependent samples t-tests for each group. Between-group differences in activation for left and right hemispheric networks were assessed with unequal variance t-tests.

Lastly, to assess the effect of lesion size on task-driven activation in the right hemisphere, we performed an additional whole-brain linear regression analysis that was restricted to the right hemisphere and included only total lesion volume as a predictor. Post-hoc moderation analyses were performed for right hemisphere clusters that showed significant positive correlations between activation magnitudes and lesion volume in order to assess whether activity in these regions might show different relationships to language measures for patients with smaller vs. larger lesions. For each identified cluster, three separate multiple regression analyses (one for each language measure) were performed that each included mean activation magnitudes for that cluster, total lesion volume (entered as a proportion of the maximum lesion volume to improve parameter estimate interpretability), and the interaction term between activation and lesion volume. For these post-hoc analyses, only the interaction effects were of interest, since they would indicate whether the effect of activity in each cluster on language performance varied as a function of lesion volume.

Statistical tests were two-tailed and significance thresholds were set as follows. Results for group comparisons and for each set of ROI-based analyses were considered significant if they survived a Bonferroni-Holm step-down correction procedure to control the FWE at 0.05 across each set of tests, since this method provides good protection against Type I errors and better power than standard Bonferroni correction [Aickin and Gensler, 1996]. T-contrast maps for the effects of interest from each of the whole-brain multiple regression analysis were thresholded at $p < 0.01$, uncorrected at the voxel level and multiple comparisons corrected at the cluster level to control the cluster-wise FWE at 0.01 ($k_{crit} = 126$ voxels, as determined by 1000 Monte Carlo simulations) for each contrast. Since power is often lower for analyses of moderation [Jaccard et al., 1990], the *post-hoc* moderation analyses were multiple comparisons corrected using a more lenient False Discovery Rate (FDR) correction threshold of 0.10 [Benjamini and Hochberg, 1995] computed across the interaction term p -values for all moderation models.

Results

Behavioral differences between patients and controls

Patients performed more poorly on language tasks than controls (in-scanner SD % correct: $t_{74.77}=-4.71, p<0.001$, corrected; BNT: $t_{43.38}=-6.80, p<0.001$, corrected; fluency: $t_{82.28}=-13.44, p<0.001$, corrected). Summary statistics are shown in Figure 2B.

Region of interest behavioral correlations

The semantic networks recruited by each group are shown in Figure 2C. Cluster peak co-ordinates and statistics for regions activated by each group are provided in Supplemental Tables 2-3. Controls showed significantly higher levels of activation in the canonical semantic network than patients ($t_{67.72}=3.98, p<0.001$, corrected). Total lesion volume showed negative relationships with each of the language measures (in-scanner SD correct: $r=-0.22, p=0.19$, corrected; fluency: $r=-0.58, p<0.001$, corrected; naming: $r=-0.49, p=0.004$, corrected), and also with mean activation in the canonical semantic network ($r=-0.27, p=0.15$, corrected). The partial correlation analyses revealed significant positive relationships between activity within the canonical semantic network and in-scanner performance on the SD task (partial $r=0.47, p=0.008$, corrected), out-of-scanner performance on the fluency measure (partial $r=0.62, p<0.001$, corrected), and out-of-scanner performance on the naming measure (partial $r=0.49, p=0.005$, corrected) that were linearly independent of the effects of total lesion volume (Figure 2D). Relationships between canonical network activation and in-scanner performance on the SD task ($r=0.51, p=0.005$, corrected), out-of-scanner performance on the fluency measure ($r=0.65, p<0.001$, corrected), and out-of-scanner performance on the naming measure ($r=0.55, p=0.001$, corrected) were stronger without lesion volume control.

Whole-brain behavioral correlations

The results for the whole-brain multiple regressions for each language measure that included total lesion volume as a covariate are shown in (Figure 3A). Cluster peak locations and statistics for each whole-brain regression are provided in Supplemental Tables 4-6. Figure 3B shows regions that showed positive relationships between activation and performance on all three language measures, and Figure 3C shows regions that showed positive relationships between activation and any of the language measures along with the canonical semantic network identified in healthy controls. Whole-brain

analyses repeated without including lesion volume as a covariate showed very similar results (Supplemental Tables 7-9).

Hemispheric correlations

We next assessed relationships between activation magnitudes in each hemisphere and the effects of lesion volume in the patient group. Correlation analyses revealed a strong positive relationship between activity in left and right hemispheric portions of the canonical semantic network without ($r=0.83, p<0.001$, corrected) and with (partial $r=0.83, p<0.001$, corrected) lesion volume control. Furthermore, activity in both the left hemispheric ($r=-0.24, p=0.11$, corrected) and right hemispheric portions of the canonical semantic network ($r=-0.31, p=0.09$, corrected) showed trend-level negative relationships to lesion volume. Results are shown in Figure 4A. Nearly identical results were obtained with (partial $r=0.81, p<0.001$, corrected) and without ($r=0.80, p<0.001$, corrected) lesion volume control using the mirrored left hemispheric network ROI. Strong positive correlations between activity in each hemispheric network were also observed for controls ($r=0.75, p<0.001$, corrected).

Neither patients ($t_{42}=0.96, p=0.34$, corrected) nor controls ($t_{42}=1.12, p=0.27$, corrected) showed significant differences in activation between left and right hemispheric networks. Patients had significantly lower activity in both the left ($t_{66.37}=-3.60, p<0.001$, corrected) and right ($t_{74.28}=-4.23, p<0.001$, corrected) hemispheric portions of the semantic network than controls.

Total lesion volume effects

The results from the whole-brain regression analysis assessing the effects of lesion volume on activation in the right hemisphere are shown in Figure 6A. Cluster statistics and peak locations are displayed in Supplemental Table 10. All of the regions showing positive relationships with lesion volume fell outside of the canonical semantic network in right frontal cortex (Figure 4B). In contrast, several of the regions showing negative relationships between activation and lesion volume overlapped with the canonical semantic network (Figure 4B).

To assess whether there was a benefit of activating of out-of-network right-hemisphere regions for patients with large lesions, we performed additional post-hoc regression analyses to assess whether there lesion size might moderate the effect of activity in each right hemispheric cluster showing positive correlations to total lesion volume (hot clusters in Figure 4B). This revealed significant interactions between lesion volume and right SMA activation for the fluency ($t_{39}=2.97$, FDR_p = 0.04) and naming ($t_{39}=2.82$, FDR_p = 0.04) measures (Figure 4C), and between lesion volume and right IFG pars opercularis activation for the fluency ($t_{39}=2.50$, FDR_p = 0.07) measure. For each of the observed interaction effects, higher levels of activation in the right hemispheric cluster was associated with lower language test scores for patients with smaller lesions, but with higher language test scores for patients with larger lesions (Figure 4C).

Discussion

Functional neuroimaging studies of post-stroke aphasia are foundational to theories of language recovery after stroke, but this theoretical foundation is primarily composed of small studies. To address this shortcoming and assess the validity of current theory of recovery, we tested what we consider to be its primary prediction – that successful long-term language recovery depends on the preservation and/or restoration of language processing in canonical language networks. Importantly, we tested this prediction in the largest sample of post-stroke aphasia patients studied to date in the functional neuroimaging literature, and utilized statistical controls to reduce the potential for confounding effects of lesion volume on imaging-behavior relationships. We also attempted to bring clarity to a contested issue in the literature – how language task-driven activity in the unaffected right hemisphere relates to left hemispheric damage and function. Finally, we tested whether the recruitment of out-of-network right hemispheric regions by patients with larger lesions might reflect beneficial compensation.

Canonical networks in both hemispheres support language processing

Drawing from the broader functional neuroimaging literature of language recovery after stroke, we expected that activation of the canonical semantic network for language processing would positively predict language functions in chronic patients. The

results of both our ROI-based and whole-brain analyses matched this expectation, and indicate that activation of the canonical semantic network is a moderate-to-strong predictor of language function in chronic patients (Figures 2 and 3). Indeed, our whole-brain analyses revealed that positive relationships between task-driven activation and language test performance were primarily localized within or adjacent to the canonical network (Figure 3). Importantly, because we used statistical controls to account for lesion volume effects, our results are not likely to be driven by differences in lesion size or overall damage to the network among patients. Thus, our results corroborate the general implications of previous functional neuroimaging studies of language outcomes in patients with LMCA stroke [Fridriksson et al., 2010; Heiss et al., 1999; Karbe et al., 1998; van Oers et al., 2010; Saur et al., 2006], and support the emphasis of current theory on the role of canonical language networks in successful long-term language recovery after stroke.

Co-activation of left and right hemispheric networks and right hemispheric effects of lesion volume

Based on the model of language recovery after stroke proposed by Heiss and Thiel (2006), we also expected that patients with lower levels of activation in the left hemispheric network would show higher levels of activation in the right hemispheric network, and that activation in the right hemispheric network would positively correlate with left hemispheric lesion volume. However, our results did not bear out this prediction. Rather, we found that across patients, activation magnitude in the right hemispheric network positively correlated with activation magnitude in the left hemispheric network and negatively correlated with lesion volume (Figure 4A). While Heiss and Thiel (2006) acknowledge that their model may not be valid for all language functions, our findings suggest that these right hemispheric portions of canonical language networks likely support various aspects of residual language function in chronic patients independently of left hemisphere damage. This conclusion is supported by other recent evidence, such as findings that measures of grey matter [Xing et al., 2015] and white matter [Pani et al., 2016] in specific right hemispheric regions positively correlate with language abilities in chronic patients. A basic role of certain right hemispheric

regions in language processing after stroke is also consistent with findings that right hemispheric activation during semantic decision [Donnelly et al., 2011], semantic comprehension [van Ettinger-Veenstra et al., 2010], sentence completion (Van Ettinger-Veenstra et al., 2012), and word fluency tasks [Van Ettinger-Veenstra et al., 2012] correlates with various measures of language function in healthy individuals.

Based on a meta-analysis of 12 functional neuroimaging studies of chronic aphasia patients, Turkeltaub and colleagues (2011) proposed that activity in most right hemispheric regions, with the notable exception of the IFG pars triangularis, reflects either compensatory recruitment or co-activation with homotopic areas in the left hemisphere. However, our findings suggests that activity in right hemispheric homologues to task-relevant left hemispheric regions may primarily reflect co-activation rather than compensation for left hemispheric damage. The finding that larger lesions were associated with reduced activity in and adjacent to several right hemispheric regions contained within the canonical semantic network, including areas in the right anterior temporal lobe, right cerebellum, and right thalamus/basal ganglia (Figure 4B), supports this conclusion.

In addition, patients with larger lesions showed increased activity in several right frontal areas, including the right inferior frontal gyrus opercularis and supplementary motor area, that were not part of the canonical semantic network (Figure 4B). Activity in the right IFG pars opercularis and right SMA showed relationships to out-of-scanner language measures that differed in direction between patients with larger vs. smaller lesions (Figure 4C). Since high activity in these regions was associated with poorer performance for patients with smaller lesions (Figure 4C), it is possible that activity in these regions interferes with the functions of task-relevant areas when canonical regions are intact, but supports residual language function when canonical regions are damaged. Alternately, high activity in these regions for patients with smaller lesions may be reflective of focal damage to critical left hemisphere areas that impede the restoration of canonical network function during recovery. Based on evidence that both the right IFG and right SMA support language processing during early recovery, but show reduced involvement in later stages when canonical networks are recovered [Saur et al., 2006], we consider this to be most likely. If this is the case, the identification of such critical regions

by future studies could provide important insights into the factors contributing to poor long-term language recovery after stroke.

A common network supporting comprehension, naming, and fluency

Activity in a subset of regions (shown in Figure 3B) correlated positively with performance on all of the language measures, suggesting that this set of regions may support processes critical for language processing after stroke. This set of regions included the left dorsal anterior superior frontal gyrus, the left angular gyrus/superior lateral occipital gyrus, bilateral precuneus and posterior cingulate gyri, bilateral parahippocampal and fusiform gyri, and the right temporal pole. These regions are commonly associated with the default mode network [Dosenbach et al., 2007; Fox et al., 2005; Raichle et al., 2001; Raichle and Snyder, 2007; Vincent et al., 2008], and several (i.e. left angular gyrus, left anterior superior frontal gyrus, bilateral posterior cingulate gyri, left parahippocampal gyrus) have been previously suggested to form a core “conceptual network” that is involved in both explicit semantic processing and ongoing manipulations of memory representations in the absence of explicit tasks [Binder et al., 1999; Leech and Sharp, 2014]. Notably, the posterior cingulate, precuneus, and angular gyrus are functionally connected to parahippocampal cortex and co-activate with parahippocampal areas during memory retrieval [Sestieri et al., 2011]. The angular gyrus [Uddin et al., 2010] and posterior cingulate gyrus [Greicius et al., 2009] also possess direct structural connections to medial temporal lobe structures such as the hippocampus that play a critical role in memory. Speculatively, since each of the language measures utilized in this study involved a memory component (e.g. recalling facts about animals for the in-scanner semantic decision task, recalling words that begin with a given letter or fit a given category for the COWAT/SFT, and recalling names of visual objects for the BNT), it is possible that activity in these regions reflects their role in supporting memory access and manipulation.

Additionally, the right anterior temporal lobe has previously been reported to support auditory verbal comprehension in patients with damage to left posterior temporal areas, and may represent an independent module capable of auditory language processing when left posterior temporal structures are compromised [Crinion and Price, 2005].

When connectivity between left and right anterior temporal areas is preserved, left frontal access to inputs processed by the right anterior temporal lobe may provide a compensatory mechanism for achieving top-down modulations (e.g. selection or integration) of semantic content via inter-hemispheric pathways [Warren et al., 2009]. In addition, medial posterior default mode regions frequently interact with elements of other functional networks [de Pasquale et al., 2012] and possess diverse structural connections to language-relevant cortical (i.e. inferior parietal, superior temporal, anterior cingulate, and supplementary/pre-motor cortices) and subcortical (including the striatum and multiple thalamic nuclei) areas whose connections may be disrupted by LMCA stroke [Cavanna and Trimble, 2006; Greicius et al., 2009]. Thus, this set of regions could potentially act to relay information among surviving language areas when primary pathways are affected by stroke, providing a potential “back-up” interface among bilateral frontal, temporal, and parietal areas to support manipulations of memory representations and/or speech inputs when canonical cortico-cortical pathways (e.g. the arcuate fasciculus) are no longer viable. While plausible, this should be regarded as speculation, as delineating the precise roles these regions play in supporting language processing after stroke is beyond the scope of this study.

Conclusions

In conclusion, this study aimed to test current theories of language recovery after stroke and bring clarity to discrepancies in the literature. Our results confirm the prediction that fMRI activation in the canonical semantic network predicts performance on multiple measures of language function in chronic patients independently of lesion volume effects, and reveal a core set of default mode regions that likely play a key role in supporting basic aspects of residual language functions in the years after stroke. Our results also suggest that left and right hemispheric portions of the semantic network co-activate to accomplish language processing after stroke, contrary to the notion that activity in right hemispheric homologues of the left hemispheric network is up-regulated to compensate for damage to the left hemispheric network. In contrast, our results suggest that patients with the most damage to the left hemispheric network recruit specific right hemispheric areas that have been previously shown to play a primary role in supporting

early recovery. We suspect that these regions may support top-down selection or motor aspects of residual language function during the chronic stage in these patients. The findings described here emphasize the importance of canonical language networks for supporting long-term language recovery after stroke, clarify the contributions of in- and out- of network right hemispheric areas to language recovery and their relationships to left hemisphere damage, and provide a more stable foundation for future studies of language recovery after stroke.

Acknowledgements

Amber Martin

Christi Banks

NIH R01 HD068488

NIH R01 NS048281

References

- Aickin M, Gensler H (1996): Adjusting for multiple testing when reporting research results: The Bonferroni vs Holm methods. *Am J Public Health* 86:726–728.
- Allendorfer J, Kissela B, Holland S, Szaflarski J (2012): Different patterns of language activation in post-stroke aphasia are detected by overt and covert versions of the verb generation fMRI task. *Med Sci Monit* 18.
- Benjamini Y, Hochberg Y (1995): Controlling the False Discovery Rate: A Practical and Powerful Approach to Multiple Testing. *J R Stat Soc Ser B* 57:289–300.
- Binder JR, Frost J a, Hammeke T a, Cox RW, Rao SM, Prieto T (1997): Human brain language areas identified by functional magnetic resonance imaging. *J Neurosci* 17:353–362.
- Binder J, Frost J, Hammeke T, Bellgowan PSF, Rao SM, Cox RW (1999): Conceptual processing during the conscious resting state: A functional MRI study. *J Cogn Neurosci* 11:80–93.
- Butler RA, Lambon Ralph MA, Woollams AM (2014): Capturing multidimensionality in stroke aphasia: mapping principal behavioural components to neural structures.

Brain:3248–3266.

Cavanna AE, Trimble MR (2006): The precuneus: a review of its functional anatomy and behavioural correlates. *Brain* 129:564–83.

Charidimou A, Kasselimis D, Varkanitsa M, Selai C, Potagas C, Evdokimidis I (2014): Why is it difficult to predict language impairment and outcome in patients with aphasia after stroke? *J Clin Neurol* 10:75–83.

Cheng B, Forkert ND, Zavaglia M, Hilgetag CC, Golsari A, Siemonsen S, Fiehler J, Pedraza S, Puig J, Cho T-H, Alawneh J, Baron J-C, Ostergaard L, Gerloff C, Thomalla G (2014): Influence of Stroke Infarct Location on Functional Outcome Measured by the Modified Rankin Scale. *Stroke* 45:1695–1702.

Crinion J, Price CJ (2005): Right anterior superior temporal activation predicts auditory sentence comprehension following aphasic stroke. *Brain* 128:2858–71.

Donnelly KM, Allendorfer JB, Szaflarski JP (2011): Right hemispheric participation in semantic decision improves performance. *Brain Res* 1419:105–116.

Dosenbach NU, Fair DA, Miezin FM, Cohen AL, Wenger KK, Dosenbach R AT, Fox MD, Snyder AZ, Vincent JL, Raichle ME, Schlaggar BL, Petersen SE (2007): Distinct brain networks for adaptive and stable task control in humans. *Proc Natl Acad Sci* 104:11073–8.

Eaton KP, Szaflarski JP, Altaye M, Ball AL, Kissela BM, Banks C, Holland SK (2008): Reliability of fMRI for studies of language in post-stroke aphasia subjects. *Neuroimage* 41:311–22.

van Ettinger-Veenstra HM, Ragnehed M, Hällgren M, Karlsson T, Landtblom A-M, Lundberg P, Engström M (2010): Right-hemispheric brain activation correlates to language performance. *Neuroimage* 49:3481–8.

Van Ettinger-Veenstra H, Ragnehed M, McAllister A, Lundberg P, Engström M (2012): Right-hemispheric cortical contributions to language ability in healthy adults. *Brain Lang* 120:395–400.

Fox MD, Snyder AZ, Vincent JL, Corbetta M, Van Essen DC, Raichle ME (2005): The human brain is intrinsically organized into dynamic, anticorrelated functional networks. *Proc Natl Acad Sci U S A* 102:9673–8.

Fridriksson J, Bonilha L, Baker JM, Moser D, Rorden C (2010): Activity in preserved left

- hemisphere regions predicts anomia severity in aphasia. *Cereb Cortex* 20:1013–9.
- Friston KJ, Holmes AP, Worsley KJ, Poline J-P, Frith CD, Frackowiak RSJ (1995): Statistical parametric maps in functional imaging: A general linear approach. *Hum Brain Mapp* 2:189–210.
- Greicius MD, Supekar K, Menon V, Dougherty RF (2009): Resting-state functional connectivity reflects structural connectivity in the default mode network. *Cereb Cortex* 19:72–8.
- Griffis JC, Nenert R, Allendorfer JB, Szaflarski JP (2016a): Interhemispheric Plasticity following Intermittent Theta Burst Stimulation in Chronic Poststroke Aphasia. *Neural Plast* 2016:20–23.
- Griffis JC, Allendorfer JB, Szaflarski JP (2016b): Voxel-based Gaussian naïve Bayes classification of ischemic stroke lesions in individual T1-weighted MRI scans. *J Neurosci Methods* 257:97–108.
- Hartwigsen G, Saur D, Price CJ, Ulmer S, Baumgaertner A, Siebner HR (2013): Perturbation of the left inferior frontal gyrus triggers adaptive plasticity in the right homologous area during speech production. *Proc Natl Acad Sci U S A* 110:16402–7.
- Heiss W, Thiel A (2006): A proposed regional hierarchy in recovery of post-stroke aphasia. *Brain Lang* 98:118–23.
- Heiss WD, Kessler J, Thiel A, Ghaemi M, Karbe H (1999): Differential capacity of left and right hemispheric areas for compensation of poststroke aphasia. *Ann Neurol* 45:430–438.
- Jaccard J, Wan CK, Turrisi R (1990): The Detection and Interpretation of Interaction Effects Between Continuous Variables in Multiple Regression. *Multivariate Behav Res* 25:467–478.
- Kaplan E, Goodglass H, Weintraub S, Segal O, van Loon-Vervoorn A (2001): Boston naming test. Pro-ed.
- Karbe H, Thiel A, Weber-luxenburger G, Kessler J, Heiss W (1998): Brain Plasticity in Poststroke Aphasia : What Is the Contribution of the Right Hemisphere? *Brain Lang* 230:215–230.
- Karnath HO, Berger MF, Kuker W, Rorden C (2004): The anatomy of spatial neglect based on voxelwise statistical analysis: A study of 140 patients. *Cereb Cortex*

14:1164–1172.

- Kozora E, Cullum CM (1995): Generative naming in normal aging: Total output and qualitative changes using phonemic and semantic constraints. *Clin Neuropsychol* 9:313–320.
- Kümmerer D, Hartwigsen G, Kellmeyer P, Glauche V, Mader I, Klöppel S, Suchan J, Karnath HO, Weiller C, Saur D (2013): Damage to ventral and dorsal language pathways in acute aphasia. *Brain* 136:619–629.
- Lazar RM, Speizer AE, Festa JR, Krakauer JW, Marshall RS (2008): Variability in language recovery after first-time stroke. *J Neurol Neurosurgery, Psychiatry* 79:530–534.
- Leech R, Sharp DJ (2014): The role of the posterior cingulate cortex in cognition and disease. *Brain* 137:12–32.
- Lezak MD, Howieson DB, Loring DW, Hannay JH, Fischer JS (1995): *Neuropsychological assessment* (3) Oxford University Press. New York.
- Maas MB, Lev MH, Ay H, Singhal AB, Greer DM, Smith WS, Harris GJ, Halpern EF, Koroshetz WJ, Furie KL (2012): The Prognosis for Aphasia in Stroke. *J Stroke Cerebrovasc Dis* 21:350–357.
- Mattioli F, Ambrosi C, Mascaro L, Scarpazza C, Pasquali P, Frugoni M, Magoni M, Biagi L, Gasparotti R (2014): Early aphasia rehabilitation is associated with functional reactivation of the left inferior frontal gyrus: a pilot study. *Stroke* 45:545–52.
- Mazaika PK, Whitfield S, Cooper JC (2005): Detection and repair of transient artifacts in fMRI data. *Neuroimage* 26:S36.
- Meinzer M, Beeson PM, Cappa S, Crinion J, Kiran S, Saur D, Parrish T, Crosson B, Thompson CK (2013): Neuroimaging in aphasia treatment research: consensus and practical guidelines for data analysis. *Neuroimage* 73:215–24.
- Meltzer JA, Wagage S, Ryder J, Solomon B, Braun AR (2013): Adaptive significance of right hemisphere activation in aphasic language comprehension. *Neuropsychologia* 51:1248–1259.
- van Oers CMM, Vink M, van Zandvoort MJE, van der Worp HB, de Haan EHF, Kappelle LJ, Ramsey NF, Dijkhuizen RM (2010): Contribution of the left and right

- inferior frontal gyrus in recovery from aphasia. A functional MRI study in stroke patients with preserved hemodynamic responsiveness. *Neuroimage* 49:885–93.
- Oldfield RC (1971): the Assessment and Analysis of Handedness: the Edinburgh Inventory. *Neuropsychologia* 9:97–113.
- Pani E, Zheng X, Wang J, Norton A, Schlaug G (2016): Right hemisphere structures predict poststroke speech fluency. *Neurology* 86:1574–1581.
- de Pasquale F, Della Penna S, Snyder AZ, Marzetti L, Pizzella V, Romani GL, Corbetta M (2012): A cortical core for dynamic integration of functional networks in the resting human brain. *Neuron* 74:753–64.
- Pedersen P (1995): Aphasia in acute stroke: incidence, determinants, and recovery. *Ann Neurol* 38:659–666.
- Raboyeau G, De Boissezon X, Marie N, Balduyck S, Puel M, Bézy C, Démonet JF, Cardebat D (2008): Right hemisphere activation in recovery from aphasia: Lesion effect or function recruitment? *Neurology* 70:290–298.
- Raichle ME, MacLeod AM, Snyder AZ, Powers WJ, Gusnard D a, Shulman GL (2001): A default mode of brain function. *Proc Natl Acad Sci U S A* 98:676–82.
- Raichle ME, Snyder AZ (2007): A default mode of brain function: a brief history of an evolving idea. *Neuroimage* 37:1083–90; discussion 1097–9.
- Ripollés P, Marco-Pallarés J, de Diego-Balaguer R, Miró J, Falip M, Juncadella M, Rubio F, Rodriguez-Fornells A (2012): Analysis of automated methods for spatial normalization of lesioned brains. *Neuroimage* 60:1296–306.
- Rorden C, Karnath H-O (2004): Using human brain lesions to infer function: a relic from a past era in the fMRI age? *Nat Rev Neurosci* 5:813–819.
- Rosen HJ, Petersen SE, Linenweber MR, Snyder a Z, White D a, Chapman L, Dromerick AW, Fiez JA, Corbetta MD (2000): Neural correlates of recovery from aphasia after damage to left inferior frontal cortex. *Neurology* 55:1883–1894.
- Saur D, Hartwigsen G (2012): Neurobiology of language recovery after stroke: lessons from neuroimaging studies. *Arch Phys Med Rehabil* 93:S15–25.
- Saur D, Lange R, Baumgaertner A, Schraknepper V, Willmes K, Rijntjes M, Weiller C (2006): Dynamics of language reorganization after stroke. *Brain* 129:1371–84.
- Schwartz MF, Kimberg DY, Walker GM, Faseyitan O, Brecher A, Dell GS, Coslett HB

- (2009): Anterior temporal involvement in semantic word retrieval: voxel-based lesion-symptom mapping evidence from aphasia. *Brain* 132:3411–27.
- Seghier ML, Ramlackhansingh A, Crinion J, Leff AP, Price CJ (2008): Lesion identification using unified segmentation-normalisation models and fuzzy clustering. *Neuroimage* 41:1253–1266.
- Sestieri C, Corbetta M, Romani GL, Shulman GL (2011): Episodic memory retrieval, parietal cortex, and the default mode network: functional and topographic analyses. *J Neurosci* 31:4407–20.
- Slotnick SD, Moo LR, Segal JB, Hart J (2003): Distinct prefrontal cortex activity associated with item memory and source memory for visual shapes. *Cogn Brain Res* 17:75–82.
- Szaflarski JP, Allendorfer JB, Banks C, Vannest J, Holland SK (2013): Recovered vs. not-recovered from post-stroke aphasia: the contributions from the dominant and non-dominant hemispheres. *Restor Neurol Neurosci* 31:347–60.
- Szaflarski JP, Holland SK, Jacola LM, Lindsell C, Privitera MD, Szaflarski M (2008): Comprehensive presurgical functional MRI language evaluation in adult patients with epilepsy. *Epilepsy Behav* 12:74–83.
- Szaflarski JP, Vannest J, Wu SW, DiFrancesco MW, Banks C, Gilbert DL (2011): Excitatory repetitive transcranial magnetic stimulation induces improvements in chronic post-stroke aphasia. *Med Sci Monit* 17:CR132–9.
- Thiel A, Schumacher B, Wienhard K, Gairing S, Kracht LW, Wagner R, Haupt WF, Heiss W-D (2006): Direct demonstration of transcallosal disinhibition in language networks. *J Cereb Blood Flow Metab* 26:1122–7.
- Turkeltaub PE, Messing S, Norise C, Hamilton RH (2011): Are networks for residual language function and recovery consistent across aphasic patients? *Neurology* 76:1726–34.
- Uddin LQ, Supekar K, Amin H, Rykhlevskaia E, Nguyen DA, Greicius MD, Menon V (2010): Dissociable connectivity within human angular gyrus and intraparietal sulcus: evidence from functional and structural connectivity. *Cereb Cortex* 20:2636–46.
- Vincent JL, Kahn I, Snyder AZ, Raichle ME, Buckner RL (2008): Evidence for a

frontoparietal control system revealed by intrinsic functional connectivity. *J Neurophysiol* 100:3328–42.

Warren JE, Crinion JT, Lambon Ralph MA, Wise RJS (2009): Anterior temporal lobe connectivity correlates with functional outcome after aphasic stroke. *Brain* 132:3428–42.

Winhuisen L, Thiel A, Schumacher B, Kessler J, Rudolf J, Haupt WF, Heiss WD (2005): Role of the contralateral inferior frontal gyrus in recovery of language function in poststroke aphasia: a combined repetitive transcranial magnetic stimulation and positron emission tomography study. *Stroke* 36:1759–63.

Winhuisen L, Thiel A, Schumacher B, Kessler J, Rudolf J, Haupt WF, Heiss WD (2007): The right inferior frontal gyrus and poststroke aphasia: a follow-up investigation. *Stroke* 38:1286–92.

Xing S, Lacey EH, Skipper-Kallal LM, Jiang X, Harris-Love ML, Zeng J, Turkeltaub PE (2015): Right hemisphere grey matter structure and language outcomes in chronic left hemisphere stroke. *Brain*:awv323.

Yarkoni T (2009): Big Correlations in Little Studies: Inflated fMRI Correlations Reflect Low Statistical Power-Commentary on Vul et al. (2009). *Perspect Psychol Sci* 4:294–298.

Yarnell P, Monroe P, Sobel L (1976): Aphasia outcome in stroke: a clinical neuroradiological correlation. *Stroke* 7:516–522.

Yongsheng Z, Kimberg D, Coslett H, Schwartz M, Wang Z (2014): Multivariate lesion-symptom mapping using support vector regression. *Hum Brain Mapp* 35:997.

Tables

Table 1. Participant demographics

Group	N	Age	Sex	Handedness
Patients	43	53 (15)	25 M	0.85 (0.43)
Controls	43	54(14)	23 M	0.80 (0.41)

**Mean (SD) are shown for age/handedness; M-Male*

Figures

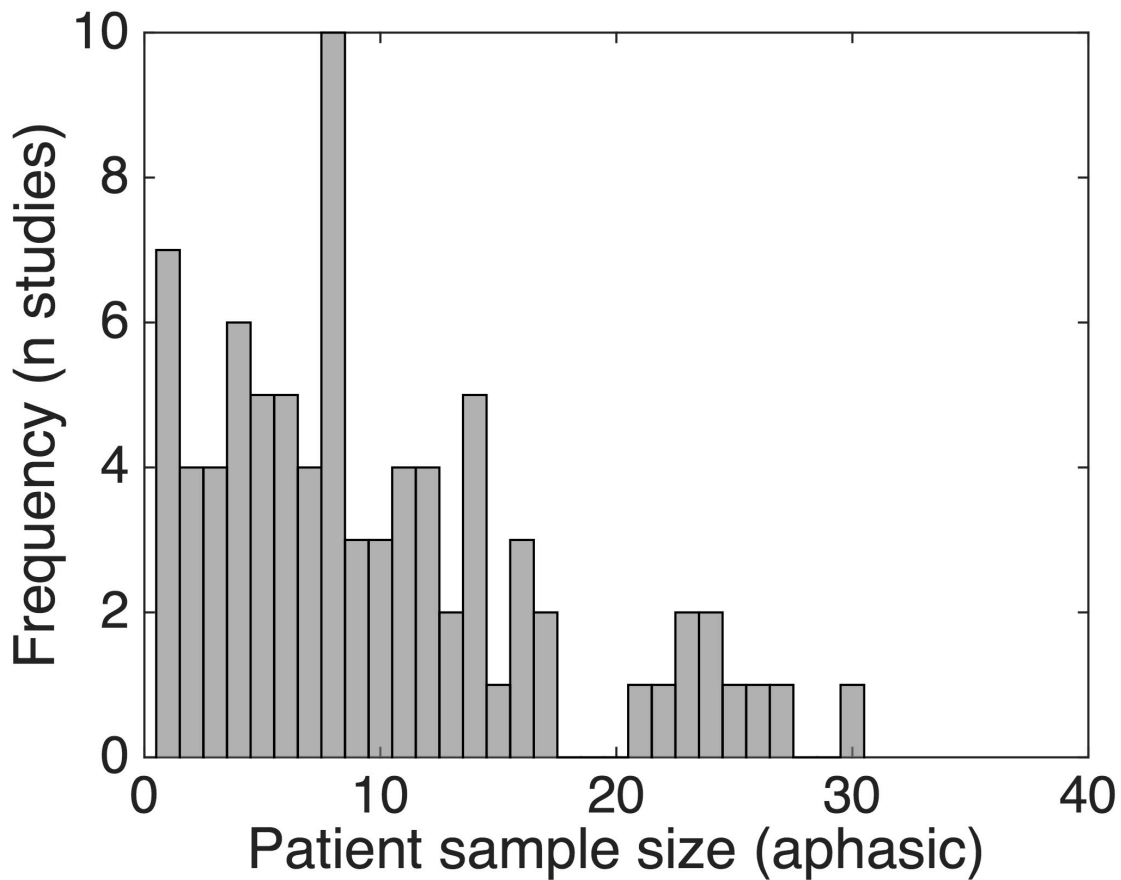


Figure 1. Sample sizes in the functional neuroimaging literature of post-stroke aphasia. Histogram illustrating frequencies of different sample sizes across 82 functional neuroimaging studies of aphasia published since 1995. Bins correspond to single integer values. The average sample size was 9.76, with a standard deviation of 7.05. The single largest sample was 30 patients. 67 (82%) of studies had samples sizes less than or equal to 15 patients, and 72 (88%) of studies had sample sizes less than or equal to 20 patients. Individual study sample sizes and neuroimaging modalities are provided in Supplementary Table 1, and the full reference list is also provided in Supplementary Material 1.

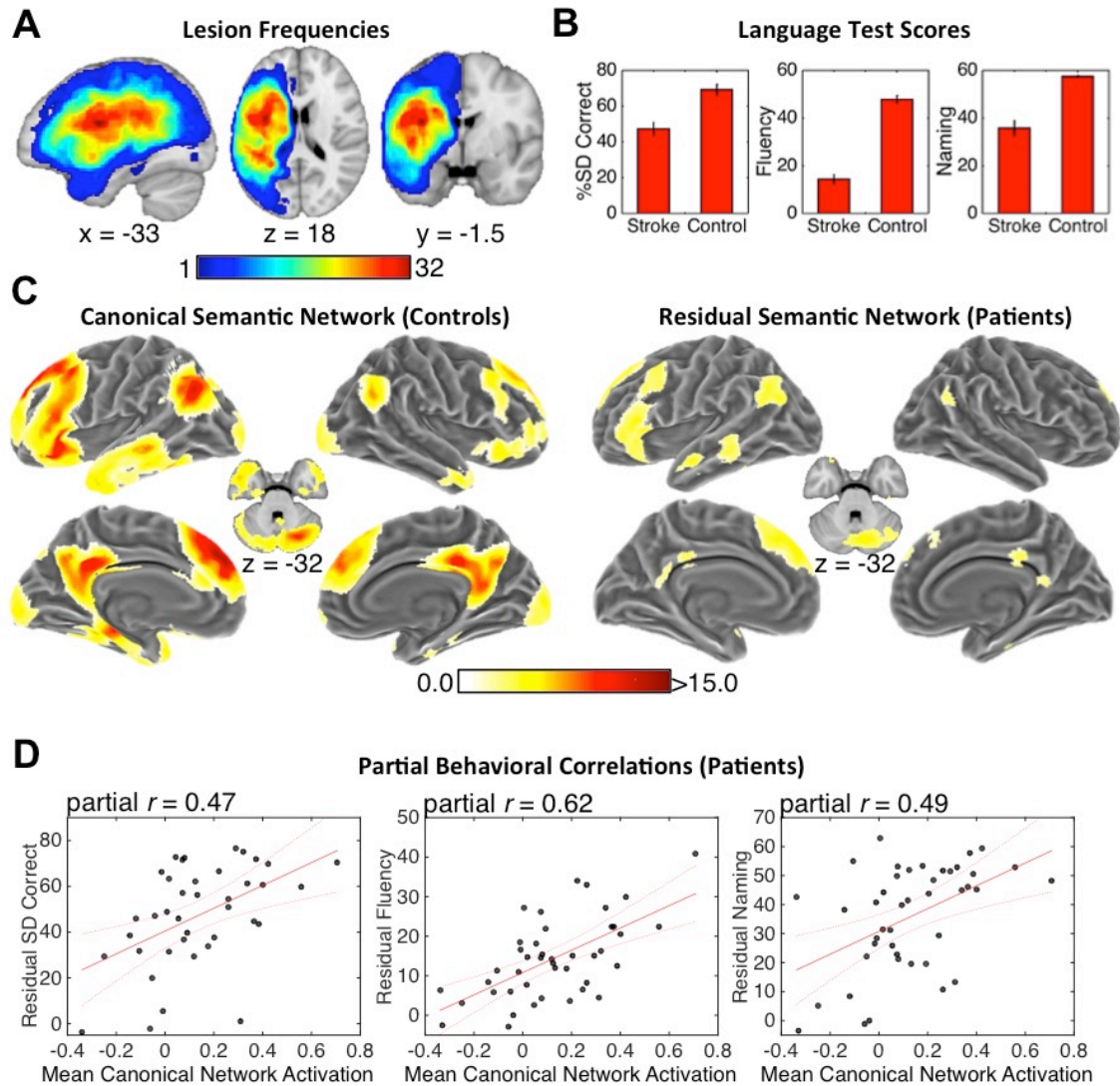


Figure 2. Data characterization and partial behavioral correlation results. **A.** Lesion frequencies across all 43 patients. Minimum colorbar values indicate voxels lesioned in only 1 patient, and maximum colorbar values indicate voxels lesioned in 32 patients (maximum lesion overlap). **B.** Means and standard errors for stroke patients and healthy controls are shown for each language measure. **C.** Areas showing significantly more activity during the SD condition relative to the control condition in the healthy controls (left) and areas showing significantly more activity during the SD condition relative to the TD condition in the stroke patients (right). Both maps are intensity thresholded at $p < 0.01$, uncorrected and cluster-corrected at $p < 0.05$ (99 voxels). Colorbar values indicate t-statistics. Note that the canonical semantic network was defined based on the results

shown in (C, left). **D.** Scatterplots illustrating the partial correlations between the residuals for activation in the canonical semantic network region of interest (defined as activations shown for healthy controls in the left panel of C) and performance on each language measure (y-axes) after removing the effects of lesion volume. The line of best fit (red) and 95% confidence intervals (red dashes) are shown on each plot. Each relationship shown was significant at $p < 0.05$, family-wise error corrected. Note: All brain renderings are in neurological convention.

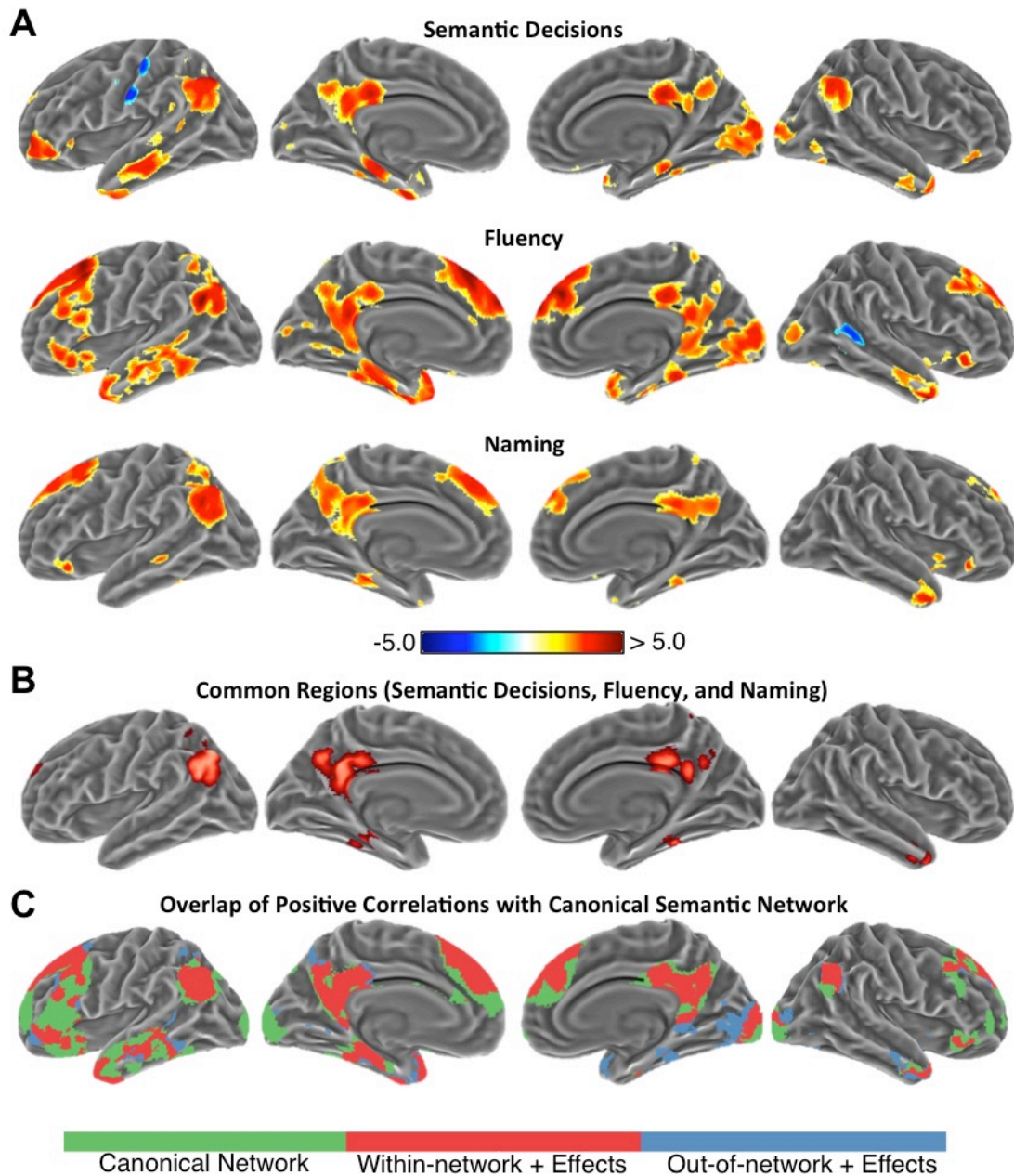


Figure 3. Whole-brain performance regression results. **A.** Positive correlations (hot colors) and negative correlations (cold colors) between task-driven activation and performance on the SD task (top) combined fluency measure (middle) and Boston Naming Test (bottom). **B.** The subset of regions showing positive correlations between SD activation and performance on all language measures are shown in red. **C.** The canonical network identified in controls is shown in green, regions within the canonical semantic network identified in healthy controls where SD activation was positively

related to performance on any language measure in patients are shown in red, and regions outside of the canonical semantic network where SD activation was positively related to performance on any language measure in patients are shown in blue. Note that the overlays shown in (C) are qualitative illustrations of how the quantitatively identified behavioral relationships in patients relate to the canonical network identified in controls, and are intended to illustrate how activity supporting residual language task performance relates to the canonical semantic network. Each map is intensity thresholded at $p < 0.01$, uncorrected and cluster-corrected at $p < 0.01$ (126 voxels). Colorbar values indicate t-statistics. All brain renderings are in neurological convention.

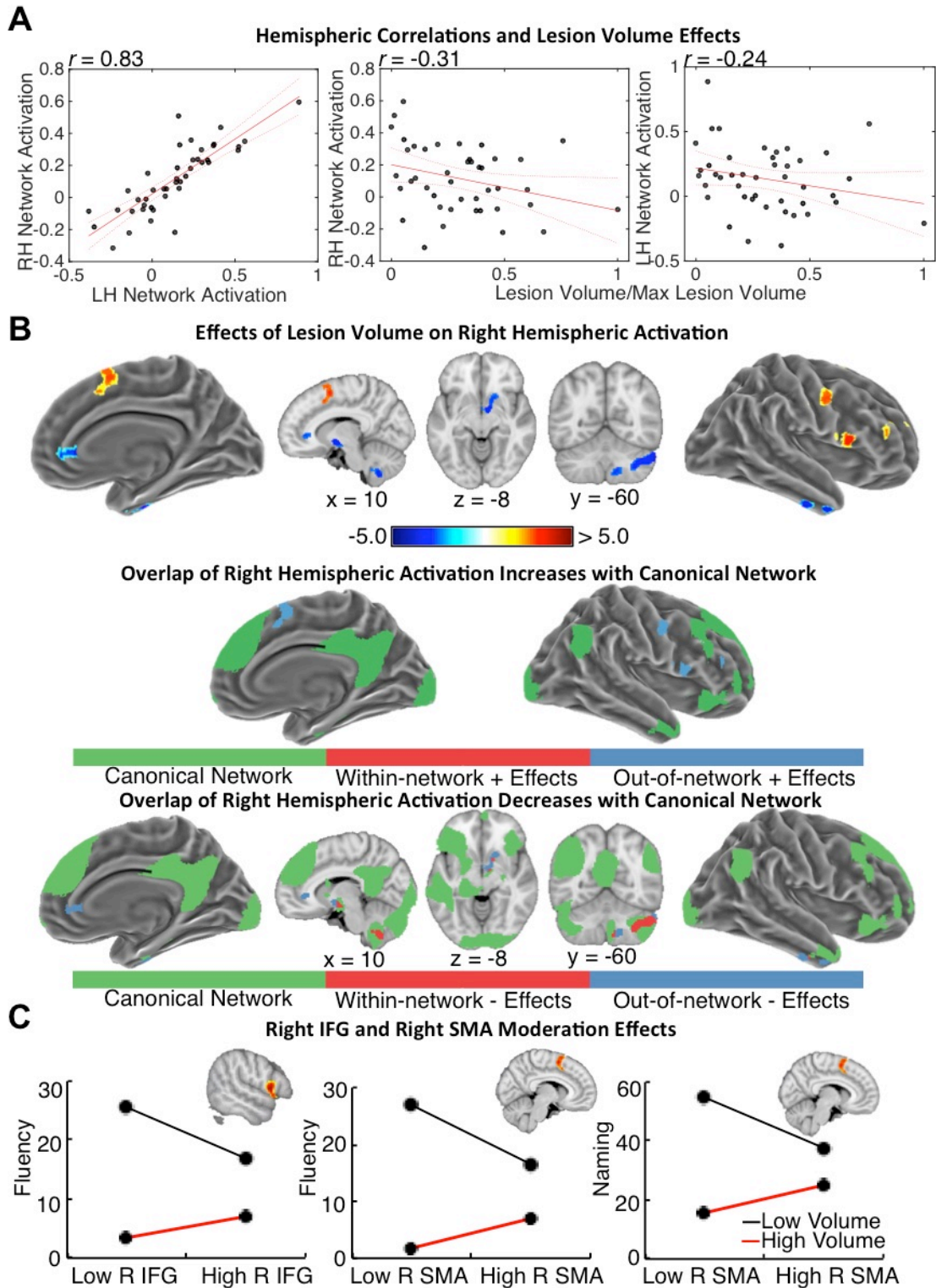


Figure 4. Relationships between left and right hemisphere activation and the effects of lesion volume. A. Scatterplots illustrating the relationship between SD-driven activity in left hemispheric (LH, x-axis) and right hemispheric (RH, y-axis) portions of the

canonical semantic network (left), the relationship between total lesion volume as a proportion of maximum lesion volume (x-axis) and activity in the right hemispheric (RH, y-axis) canonical semantic network (middle), and the relationship between total lesion volume as a proportion of maximum lesion volume (x-axis) and activity in the right hemispheric (RH, y-axis) canonical semantic network (right). **B.** Positive correlations (hot colors) and negative correlations (cold colors) between task-driven activation and lesion volume in right hemispheric areas are shown (top). The canonical semantic network (green) identified in healthy controls is shown along with out-of-network increases in activation (blue) associated with larger lesion volumes (middle); Note that there were no overlaps between regions with increased activity in patients with larger lesion volumes and the canonical semantic network. The canonical semantic network (green) identified in healthy controls is shown along with within-network (red) and out-of-network (blue) reductions in activation associated with larger lesion volumes (bottom). Note that the overlays shown in (B, middle and bottom rows) are qualitative illustrations of the quantitatively identified lesion volume effects on right hemispheric activations, and illustrate how right hemispheric activations associated with lesion volume effects relate to the canonical network in the right hemisphere. **C.** Interaction plots are shown for the moderating effects of lesion volume on the relationship between right inferior frontal gyrus (IFG) activation and fluency scores (left), right supplementary motor area (SMA) activation and fluency scores (middle), and right SMA activation and naming scores (right). Each of these relationships survived a False Discovery Rate threshold of 0.1. High and low values shown in the plots correspond to +1 and -1 standard deviations from the mean of each variable. All maps are intensity thresholded at $p < 0.01$, uncorrected and cluster-corrected at $p < 0.01$ (126 voxels). Colorbar values indicate t-statistics. Note: all brain renderings are in neurological convention.

Supplementary Material 1

Table 1. Patient sample sizes for 82 functional neuroimaging studies of aphasia published since 1995.

Study	N	Modality	Study	N	Modality
Weiller et al., 1995	6	PET	Richter et al., 2008	16	fMRI
Belin et al., 1996	7	PET	Abutalebi et al., 2009	1	fMRI
Cappa et al., 1997	8	PET	Breier et al., 2009	23	MEG
Heiss et al., 1997	6	PET	Fridriksson et al., 2009	11	fMRI
Thomas et al., 1997	11	EEG	Martin et al., 2009	2	fMRI
Desk et al., 1998	10	NIRS	Specht et al., 2009	12	PET
Karbe et al., 1998	7	PET	Warren et al., 2009	24	PET
Heiss et al., 1999	23	PET	Fridriksson et al., 2010a	15	fMRI
Miura et al., 1999	1	fMRI	Fridriksson et al., 2010b	26	fMRI
Musso et al., 1999	4	PET	Postman-Caucheteux et al., 2010	3	fMRI
Warburton et al., 1999	6	PET	Rochon et al., 2010	4	fMRI
Rosen et al., 2000	6	PET+fMRI	Saur et al., 2010	21	fMRI
Blasi et al., 2002	8	fMRI	Sharp et al., 2010	9	PET
Leger et al., 2002	1	fMRI	Thompson et al., 2010a	5	fMRI
Blank et al., 2003	14	PET	Thompson et al., 2010b	6	fMRI
Cardebat et al., 2003	8	PET	Van Oers et al., 2010	13	fMRI
Perani et al., 2003	5	fMRI	Papoutsis et al., 2011	8	fMRI
Fernandez et al., 2004	1	fMRI	Szaflarski et al., 2011a	8	fMRI
Kurland et al., 2004	2	fMRI	Szaflarski et al., 2011b	4	fMRI
Naeser et al., 2004	4	fMRI	Tyler et al., 2011	14	fMRI
Peck et al., 2004	3	fMRI	Weiduschat et al., 2011	10	PET
Zahn et al., 2004	7	fMRI	Allendorfer et al., 2012	16	fMRI
Crinion et al., 2005	17	fMRI	Fridriksson et al., 2012	30	fMRI
Crosson et al., 2005	2	fMRI	Meltzer et al., 2013	25	MEG
De Boissezon et al., 2005	7	PET	Szaflarski et al., 2013	27	fMRI
Martin et al., 2005	5	fMRI	Thompson et al., 2013	8	fMRI
Pulvermuller et al., 2005	9	EEG	Thiel et al., 2013	24	PET
Winhuisen et al., 2005	11	PET	Abel et al., 2014	14	fMRI
Meinzer et al., 2006	1	fMRI	Brownsett et al., 2014	16	fMRI
Connor et al., 2006	8	fMRI	Jarso et al., 2014	4	fMRI
Crinion et al., 2006	22	PET	Mattioli et al., 2014	12	fMRI
Fridriksson et al., 2006	3	fMRI	Mohr et al., 2014	12	fMRI
Saur et al., 2006	14	fMRI	Robson et al., 2014	12	fMRI
Bonakdarpour et al., 2007	5	fMRI	Seghier et al., 2014	1	fMRI
Fridriksson et al., 2007	3	fMRI	Van Hees et al., 2014	8	fMRI
Meinzer et al., 2007	1	fMRI	Zhu et al., 2014	13	fMRI
Winhuisen et al., 2007	9	PET	Abel et al., 2015	14	fMRI
Vitali et al., 2007	2	fMRI	Bonakdarpour et al., 2015	5	fMRI
Eaton et al., 2008	4	fMRI	Kiran et al., 2015	8	fMRI
Meinzer et al., 2008	11	fMRI	Spironelli et al., 2015	17	EEG
Raboyeau et al., 2008	10	PET	Griffis et al., 2016	8	fMRI

Supplementary Table 1 References

Abel S, Weiller C, Huber W, Willmes K, Specht K. Therapy-induced brain reorganization patterns in aphasia. *Brain* 2015; 138: 1097–112.

Abel S, Weiller C, Huber W, Willmes K. Neural underpinnings for model-oriented therapy of aphasic word production. *Neuropsychologia* 2014; 57: 154–165.

Abutalebi J, Rosa PA Della, Tettamanti M, Green DW, Cappa SF. Bilingual aphasia and language control: A follow-up fMRI and intrinsic connectivity study. *Brain Lang.* 2009; 109: 141–156.

Allendorfer J, Kissela B, Holland S, Szaflarski J. Different patterns of language activation in post-stroke aphasia are detected by overt and covert versions of the verb generation fMRI task. *Medical Science Monitor*. 2012; 18

Belin P, Van Eeckhout P, Zilbovicius M, Remy P, François C, Guillaume S, et al. Recovery from nonfluent aphasia after melodic intonation therapy: a PET study. *Neurology* 1996; 47: 1504–1511.

Blank SC, Bird H, Turkheimer F, Wise RJS. Speech production after stroke: The role of the right pars opercularis. *Ann. Neurol*. 2003; 54: 310–320.

Blasi V, Young AC, Tansy AP, Petersen SE, Snyder AZ, Corbetta M. Word retrieval learning modulates right frontal cortex in patients with left frontal damage. *Neuron* 2002; 36: 159–170.

De Boissezon X, Démonet JF, Puel M, Marie N, Raboyeau G, Albucher JF, et al. Subcortical aphasia: A longitudinal PET study. *Stroke* 2005; 36: 1467–1473.

Bonakdarpour B, Beeson PM, DeMarco AT, Rapcsak SZ. Variability in blood oxygen level dependent (BOLD) signal in patients with stroke-induced and primary progressive aphasia. *NeuroImage Clin*. 2015; 8: 87–94.

Bonakdarpour B, Parrish TB, Thompson CK. Hemodynamic response function in patients with stroke-induced aphasia: implications for fMRI data analysis. *Neuroimage* 2007; 36: 322–31.

Breier JJ, Juranek J, Maher LM, Schmadeke S, Men D, Papanicolaou AC. Behavioral and Neurophysiologic Response to Therapy for Chronic Aphasia. *Arch. Phys. Med. Rehabil*. 2009; 90: 2026–2033.

Brownsett SLE, Warren JE, Geranmayeh F, Woodhead Z, Leech R, Wise RJS. Cognitive control and its impact on recovery from aphasic stroke. *Brain* 2014; 137: 242–54.

Cappa SF, Perani D, Grassi F, Bressi F, Alberoni M, Franceschi M, et al. A PET Follow-up Study of Recovery after Stroke in Acute Aphasics. *Brain Lang*. 1997; 56: 55–67.
Cardebat D, Demonet JF, De Boissezon X, Marie N, Marie RM, Lambert J, et al. Behavioral and Neurofunctional Changes over Time in Healthy and Aphasic Subjects: A PET Language Activation Study. *Stroke* 2003; 34: 2900–2906.

Connor LT, DeShazo Braby T, Snyder AZ, Lewis C, Blasi V, Corbetta M. Cerebellar activity switches hemispheres with cerebral recovery in aphasia. *Neuropsychologia* 2006; 44: 171–7.

Crinion J, Price CJ. Right anterior superior temporal activation predicts auditory sentence comprehension following aphasic stroke. *Brain* 2005; 128: 2858–71.

Crinion JT, Warburton EA, Lambon-Ralph MA, Howard D, Wise RJS. Listening to narrative speech after aphasic stroke: The role of the left anterior temporal lobe. *Cereb. Cortex* 2006; 16: 1116–1125.

Crosson B, Moore AB, Gopinath K, White KD, Wierenga CE, Gaiefsky ME, et al. Role of the right and left hemispheres in recovery of function during treatment of intention in aphasia. *J. Cogn. Neurosci.* 2005; 17: 392–406.

Desk R, Williams L, Health K. Language-Activated Cerebral Blood Oxygenation and Hemodynamic Changes of the Left Prefrontal Cortex in Poststroke Aphasic Patients. *Stroke* 1998; 29: 12–14.

Eaton KP, Szaflarski JP, Altaye M, Ball AL, Kissela BM, Banks C, et al. Reliability of fMRI for studies of language in post-stroke aphasia subjects. *Neuroimage* 2008; 41: 311–22.

Fernandez B, Cardebat D, Demonet JF, Joseph PA, Mazaux JM, Barat M, et al. Functional MRI follow-up study of language processes in healthy subjects and during recovery in a case of aphasia. *Stroke* 2004; 35: 2171–2176.

Fridriksson J, Baker JM, Moser D. Cortical mapping of naming errors in aphasia. *Hum. Brain Mapp.* 2009; 30: 2487–2498.

Fridriksson J, Bonilha L, Baker JM, Moser D, Rorden C. Activity in preserved left hemisphere regions predicts anomia severity in aphasia. *Cereb. Cortex* 2010; 20: 1013–9.

Fridriksson J, Morrow-Odom L, Moser D, Fridriksson A, Baylis G. Neural recruitment associated with anomia treatment in aphasia. *Neuroimage* 2006; 32: 1403–1412.

Fridriksson J, Moser D, Bonilha L, Morrow-Odom KL, Shaw H, Fridriksson A, et al. Neural correlates of phonological and semantic-based anomia treatment in aphasia. *Neuropsychologia* 2007; 45: 1812–22.

Fridriksson J, Richardson JD, Fillmore P, Cai B. Left hemisphere plasticity and aphasia recovery. *Neuroimage* 2012; 60: 854–63.

Fridriksson J. Preservation and modulation of specific left hemisphere regions is vital for treated recovery from anomia in stroke. *J. Neurosci.* 2010; 30: 11558–11564.

Griffis JC, Nenert R, Allendorfer JB, Szaflarski JP. Interhemispheric Plasticity following Intermittent Theta Burst Stimulation in Chronic Poststroke Aphasia. *Neural Plast.* 2015; 2016: 20–23.

Van Hees S, McMahon K, Angwin A, de Zubicaray G, Read S, Copland DA. A functional MRI study of the relationship between naming treatment outcomes and resting

state functional connectivity in post-stroke aphasia. *Hum. Brain Mapp.* 2014; 35: 3919–31.

Heiss WD, Karbe H, Weber-Luxenburger G, Herholz K, Kessler J, Pietrzyk U, et al. Speech-induced cerebral metabolic activation reflects recovery from aphasia. *J. Neurol. Sci.* 1997; 145: 213–217.

Heiss WD, Kessler J, Thiel A, Ghaemi M, Karbe H. Differential capacity of left and right hemispheric areas for compensation of poststroke aphasia. *Ann. Neurol.* 1999; 45: 430–438.

Jarso S, Li M, Faria A, Davis C, Leigh R, Sebastian R, et al. Distinct mechanisms and timing of language recovery after stroke. *Cogn. Neuropsychol.* 2014; 0: 1–22.

Karbe H, Thiel A, Weber-luxenburger G, Kessler J, Heiss W. Brain Plasticity in Poststroke Aphasia : What Is the Contribution of the Right Hemisphere? *Brain Lang.* 1998; 230: 215–230.

Kiran S, Meier EL, Kapse KJ, Glynn PA. Changes in task-based effective connectivity in language networks following rehabilitation in post-stroke patients with aphasia. *Front. Hum. Neurosci.* 2015; 9: 1–20.

Kurland J, Naeser MA, Baker EH, Doron K, Martin PI, Seekins HE, et al. Test-retest reliability of fMRI during nonverbal semantic decisions in moderate-severe nonfluent aphasia patients. *Behav. Neurol.* 2004; 15: 87–97.

Léger A, Démonet JF, Ruff S, Aithamon B, Touyeras B, Puel M, et al. Neural substrates of spoken language rehabilitation in an aphasic patient: an fMRI study. *Neuroimage* 2002; 17: 174–183.

Martin PI, Naeser MA, Doron KW, Bogdan A, Baker EH, Kurland J, et al. Overt naming in aphasia studied with a functional MRI hemodynamic delay design. *Neuroimage* 2005; 28: 194–204.

Martin PI, Naeser MA, Ho M, Doron KW, Kurland J, Kaplan J, et al. Overt naming fMRI pre- and post-TMS: Two nonfluent aphasia patients, with and without improved naming post-TMS. *Brain Lang.* 2009; 111: 20–35.

Mattioli F, Ambrosi C, Mascaro L, Scarpazza C, Pasquali P, Frugoni M, et al. Early aphasia rehabilitation is associated with functional reactivation of the left inferior frontal gyrus: a pilot study. *Stroke.* 2014; 45: 545–52.

Meinzer M, Flaisch T, Breitenstein C, Wienbruch C, Elbert T, Rockstroh B. Functional re-recruitment of dysfunctional brain areas predicts language recovery in chronic aphasia. *Neuroimage* 2008; 39: 2038–46.

Meinzer M, Flaisch T, Obleser J, Assadollahi R, Djundja D, Barthel G, et al. Brain regions essential for improved lexical access in an aged aphasic patient: a case report. *BMC Neurol.* 2006; 6: 28.

Meinzer M, Obleser J, Flaisch T, Eulitz C, Rockstroh B. Recovery from aphasia as a function of language therapy in an early bilingual patient demonstrated by fMRI. *Neuropsychologia* 2007; 45: 1247–1256.

Meltzer JA, Wagage S, Ryder J, Solomon B, Braun AR. Adaptive significance of right hemisphere activation in aphasic language comprehension. *Neuropsychologia* 2013; 51: 1248–1259.

Miura K, Nakamura Y, Miura F, Yamada I, Takahashi M, Yoshikawa A, et al. Functional magnetic resonance imaging to word generation task in a patient with Broca's aphasia. *J. Neurol.* 1999; 246: 939–942.

Mohr B, Difrancesco S, Harrington K, Evans S, Pulvermuller F. Changes of right-hemispheric activation after constraint-induced, intensive language action therapy in chronic aphasia: fMRI evidence from auditory semantic processing1. *Front. Hum. Neurosci.* 2014; 8: 1–15.

Musso M, Weiller C, Kiebel S, Müller SP, Bülow P, Rijntjes M. Training-induced brain plasticity in aphasia. *Brain* 1999; 122 : 1781–90.

Naeser MA, Martin PI, Baker EH, Hodge SM, Sczerzenie SE, Nicholas M, et al. Overt propositional speech in chronic nonfluent aphasia studied with the dynamic susceptibility contrast fMRI method. *Neuroimage* 2004; 22: 29–41.

Van Oers C, Vink M, van Zandvoort MJE, van der Worp HB, de Haan EHF, Kappelle LJ, et al. Contribution of the left and right inferior frontal gyrus in recovery from aphasia. A functional MRI study in stroke patients with preserved hemodynamic responsiveness. *Neuroimage* 2010; 49: 885–93.

Papoutsis M, Stamatakis EA, Griffiths J, Marslen-Wilson WD, Tyler LK. Is left fronto-temporal connectivity essential for syntax? Effective connectivity, tractography and performance in left-hemisphere damaged patients. *Neuroimage* 2011; 58: 656–64.

Peck KK, Moore AB, Crosson BA, Gaiefsky M, Gopinath KS, White K, et al. Functional Magnetic Resonance Imaging before and after Aphasia Therapy: Shifts in Hemodynamic Time to Peak during an Overt Language Task. *Stroke* 2004; 35: 554–559.

Perani D, Cappa SF, Tettamanti M, Rosa M, Scifo P, Miozzo A, et al. A fMRI study of word retrieval in aphasia. *Brain Lang.* 2003; 85: 357–368.

Postman-Caucheteux WA, Birn RM, Pursley RH, Butman JA, Solomon JM, Picchioni D, et al. Single-trial fMRI shows contralesional activity linked to overt naming errors in

chronic aphasic patients. *J. Cogn. Neurosci.* 2010; 22: 1299–1318.

Pulvermüller F, Hauk O, Zohsel K, Neininger B, Mohr B. Therapy-related reorganization of language in both hemispheres of patients with chronic aphasia. *Neuroimage* 2005; 28: 481–9.

Raboyeau G, De Boissezon X, Marie N, Balduyck S, Puel M, Bézy C, et al. Right hemisphere activation in recovery from aphasia: Lesion effect or function recruitment? *Neurology* 2008; 70: 290–298.

Richter M, Miltner WHR, Straube T. Association between therapy outcome and right-hemispheric activation in chronic aphasia. *Brain* 2008; 131: 1391–1401.

Robson H, Zahn R, Keidel JL, Binney RJ, Sage K, Lambon Ralph MA. The anterior temporal lobes support residual comprehension in Wernicke's aphasia. *Brain* 2014; 137: 931–43.

Rochon E, Leonard C, Burianova H, Laird L, Soros P, Graham S, et al. Neural changes after phonological treatment for anomia: An fMRI study. *Brain Lang.* 2010; 114: 164–179.

Rosen HJ, Petersen SE, Linenweber MR, Snyder AZ, White DA, Chapman L, et al. Neural correlates of recovery from aphasia after damage to left inferior frontal cortex. *Neurology* 2000; 55: 1883–1894.

Saur D, Lange R, Baumgaertner A, Schraknepper V, Willmes K, Rijntjes M, et al. Dynamics of language reorganization after stroke. *Brain* 2006; 129: 1371–84.

Saur D, Ronneberger O, Kümmerer D, Mader I, Weiller C, Klöppel S. Early functional magnetic resonance imaging activations predict language outcome after stroke. *Brain* 2010; 133: 1252–1264.

Seghier ML, Bagdasaryan J, Jung DE, Price CJ. The Importance of Premotor Cortex for Supporting Speech Production after Left Capsular-Putaminal Damage. *J. Neurosci.* 2014; 34: 14338–14348.

Sharp DJ, Turkheimer FE, Bose SK, Scott SK, Wise RJS. Increased frontoparietal integration after stroke and cognitive recovery. *Ann. Neurol.* 2010; 68: 753–6.

Specht K, Zahn R, Willmes K, Weis S, Holtel C, Krause BJ, et al. Joint independent component analysis of structural and functional images reveals complex patterns of functional reorganisation in stroke aphasia. *Neuroimage* 2009; 47: 2057–2063.

Spironelli C, Angrilli A. Brain plasticity in aphasic patients: intra- and inter-hemispheric reorganisation of the whole linguistic network probed by N150 and N350 components. *Sci. Rep.* 2015; 5: 12541.

Szaflarski JP, Allendorfer JB, Banks C, Vannest J, Holland SK. Recovered vs. not-recovered from post-stroke aphasia: the contributions from the dominant and non-dominant hemispheres. *Restor. Neurol. Neurosci.* 2013; 31: 347–60.

Szaflarski JP, Eaton K, Ball AL, Banks C, Vannest J, Allendorfer JB, et al. Poststroke aphasia recovery assessed with functional magnetic resonance imaging and a picture identification task. *J. Stroke Cerebrovasc. Dis.* 2011; 20: 336–345.

Szaflarski JP, Vannest J, Wu SW, DiFrancesco MW, Banks C, Gilbert DL. Excitatory repetitive transcranial magnetic stimulation induces improvements in chronic post-stroke aphasia. *Med. Sci. Monit.* 2011; 17: CR132–9.

Thiel A, Hartmann A, Rubi-Fessen I, Anglade C, Kracht L, Weiduschat N, et al. Effects of noninvasive brain stimulation on language networks and recovery in early poststroke aphasia. *Stroke.* 2013; 44: 2240–6.

Thomas C, Altenmüller E, Marckmann G, Kahrs J, Dichgans J. Language processing in aphasia: Changes in lateralization patterns during recovery reflect cerebral plasticity in adults. *Electroencephalogr. Clin. Neurophysiol.* 1997; 102: 86–97.

Thompson CK, den Ouden DB, Bonakdarpour B, Garibaldi K, Parrish TB. Neural plasticity and treatment-induced recovery of sentence processing in agrammatism. *Neuropsychologia* 2010; 48: 3211–3227.

Thompson CK, Bonakdarpour B, Fix SF. Neural mechanisms of verb argument structure processing in agrammatic aphasic and healthy age-matched listeners. *J. Cogn. Neurosci.* 2010; 22: 1993–2011.

Thompson CK, Riley EA, den Ouden DB, Meltzer-Asscher A, Lukic S. Training verb argument structure production in agrammatic aphasia: Behavioral and neural recovery patterns. *Cortex* 2013; 49: 2358–2376.

Tyler LK, Marslen-Wilson WD, Randall B, Wright P, Devereux BJ, Zhuang J, et al. Left inferior frontal cortex and syntax: Function, structure and behaviour in patients with left hemisphere damage. *Brain* 2011; 134: 415–431.

Vitali P, Abutalebi J, Tettamanti M, Danna M, Ansaldo A-I, Perani D, et al. Training-induced brain remapping in chronic aphasia: a pilot study. *Neurorehabil. Neural Repair* 2007; 21: 152–60.

Warburton E, Price CJ, Swinburn K, Wise RJ. Mechanisms of recovery from aphasia: evidence from positron emission tomography studies. *J. Neurol. Neurosurg. Psychiatry* 1999; 66: 155–61.

Warren JE, Crinion JT, Lambon Ralph MA, Wise RJS. Anterior temporal lobe

connectivity correlates with functional outcome after aphasic stroke. *Brain* 2009; 132: 3428–42.

Weiduschat N, Thiel A, Rubi-Fessen I, Hartmann A, Kessler J, Merl P, et al. Effects of repetitive transcranial magnetic stimulation in aphasic stroke: a randomized controlled pilot study. *Stroke*. 2011; 42: 409–15.

Weiller C, Isensee C, Rijntjes M, Huber W, Müller S, Bier D, et al. Recovery from Wernicke's aphasia: A positron emission tomographic study. *Ann. Neurol.* 1995; 37: 723–732.

Winhuisen L, Thiel A, Schumacher B, Kessler J, Rudolf J, Haupt WF, et al. Role of the contralateral inferior frontal gyrus in recovery of language function in poststroke aphasia: a combined repetitive transcranial magnetic stimulation and positron emission tomography study. *Stroke*. 2005; 36: 1759–63.

Winhuisen L, Thiel A, Schumacher B, Kessler J, Rudolf J, Haupt WF, et al. The right inferior frontal gyrus and poststroke aphasia: a follow-up investigation. *Stroke*. 2007; 38: 1286–92.

Zahn R, Drews E, Specht K, Kemeny S, Reith W, Willmes K, et al. Recovery of semantic word processing in global aphasia: A functional MRI study. *Cogn. Brain Res.* 2004; 18: 322–336.

Zhu D, Chang J, Freeman S, Tan Z, Xiao J, Gao Y, et al. Changes of functional connectivity in the left frontoparietal network following aphasic stroke. *Front. Behav. Neurosci.* 2014; 8: 167.

Supplementary Table 2. Clusters of significant activation during semantic decisions for the control group.

Sign	Peak Location	Extent	t-value	x	y	z
Positive	L Superior Medial Gyrus	44277	14.3308	-4	46	36
	R Posterior Cingulate	44277	10.8963	2	-34	32
	L IFG (p. Orbitalis)	44277	10.6975	-36	30	-8
	L Angular Gyrus	3981	11.8496	-40	-64	36
	R Angular Gyrus	1051	8.1312	50	-60	32
	R Mid Orbital Gyrus	125	3.3213	2	66	-12

Supplementary Table 3. Clusters of significant activation during semantic decisions for the patient group.

Sign	Peak Location	Extent	t-value	x	y	z
Positive	R Cerebellum (VIII)	3519	5.1981	10	-76	-28
	R Cerebellum (IX)	3519	4.1282	8	-54	-52
	R Cerebellum (VII)	3519	3.8702	42	-66	-48
	L Superior Medial Gyrus	7349	4.9037	-2	40	56
	L IFG (p. Triangularis)	7349	4.7172	-48	28	8
	R Superior Frontal Gyrus	7349	4.0744	16	54	30
	L Middle Temporal Gyrus	253	4.409	-52	-8	-18
	L Middle Temporal Gyrus	1085	4.4082	-44	-64	28
	R Angular Gyrus	254	4.0334	54	-68	32
	Posterior Cingulate	217	3.9907	0	-32	30
	L Inferior Temporal Gyrus	585	3.9528	-60	-32	-12
	R Fusiform Gyrus	111	3.7833	40	-24	-28
	R Posterior Cingulate	265	2.9714	4	-46	14

Supplementary Table 4. Clusters with significant correlations between activation and in-scanner semantic decision performance while controlling for lesion volume.

Sign	Peak Location	Extent	t-value	x	y	z
Positive	L Angular Gyrus	1913	4.9167	-42	-68	48
	L Middle Temporal Gyrus	1913	2.5892	-50	-46	8
	Cerebellar Vermis (VII)	5291	4.8921	-2	-78	-18
	Posterior Cingulate Gyrus	5291	4.4726	0	-32	32
	L Calcarine Gyrus	5291	4.3329	4	-94	12
	Dorsal Anterior Pons	544	4.6492	0	-12	-28
	L Middle Orbital Gyrus	961	4.5543	-42	54	0
	L Middle Temporal Gyrus	785	4.4425	-68	-32	-2
	L Inferior Temporal Gyrus	671	4.3857	-32	-6	-38
	R Angular Gyrus	547	4.2227	54	-58	40
	L Parahippocampal Gyrus	457	4.0258	-22	-28	-18
	R Parahippocampal Gyrus	275	3.9305	20	-32	-20
	L Superior Frontal Gyrus	175	3.745	-20	56	32
	R IFG (p. Orbitalis)	160	3.7179	50	38	-18
	R Precuneus	211	3.6912	4	-62	66
	R Rectal Gyrus	135	3.6875	2	24	-30
	R Inferior Temporal Gyrus	153	3.6576	56	-12	-30
	R Temporal Pole	421	3.6249	36	14	-24
Negative	L Postcentral Gyrus	258	-3.4808	-60	-10	30

Supplementary Table 5. Clusters with significant correlations between activation and out-of-scanner fluency scores while controlling for lesion volume.

Sign	Peak Location	Extent	t-value	x	y	z
Positive	R Superior Medial Gyrus	7588	6.0189	2	50	38
	L Middle Frontal Gyrus	7588	5.8247	-34	18	52
	L Posterior-Medial Frontal	7588	5.1085	-4	20	66
	L Brainstem (Inf. Colliculus?)	6302	5.2447	-2	-30	-20
	L Fusiform Gyrus	6302	4.9057	-34	-18	-30
	R Cerebelum (IX)	6302	4.8778	8	-56	-38
	L Angular Gyrus	1227	5.2081	-48	-62	32
	L Posterior Cingulate	4805	4.6649	-2	-46	18
	R Cerebelum (VI)	4805	4.0471	28	-80	-14
	L Calcarine Gyrus	4805	3.6055	0	-92	6
	R Fusiform Gyrus	232	4.616	34	-18	-34
	R Medial Temporal Pole	1532	4.5911	46	6	-36
	R Middle Temporal Gyrus	1532	3.7147	68	-16	-20
	R Parahippocampal Gyrus	1532	3.685	16	-2	-30
	L IFG (p. Orbitalis)	587	4.0197	-40	24	-12
Negative	R Middle Temporal Gyrus	155	-3.3541	48	-48	2

Supplementary Table 6. Clusters with significant correlations between activation and out-of-scanner naming scores while controlling for lesion volume.

Sign	Peak Location	Extent	t-value	x	y	z
Positive	R Superior Medial Gyrus	5204	5.5202	2	54	46
	L Middle Frontal Gyrus	5204	4.494	-34	16	52
	R Posterior-Medial Frontal	5204	3.4022	6	14	74
	L Angular Gyrus	1889	4.2896	-46	-60	30
	R Inferior Temporal Gyrus	268	4.207	48	2	-34
	L Fusiform Gyrus	474	3.9476	-40	-34	-14
	R IFG (p. Orbitalis)	354	3.921	44	24	-14
	R Fusiform Gyrus	265	3.9092	16	-8	-42
	R Superior Orbital Gyrus	265	2.6356	16	14	-18
	R Cerebelum (IX)	762	3.8878	14	-46	-38
	R Precuneus	2516	3.8798	2	-66	64
	Posterior Cingulate	2516	3.5849	0	-36	32
	L Superior Parietal Lobule	2516	2.4993	-28	-56	66
	L IFG (p. Orbitalis)	202	3.8209	-42	26	-16
	L Fusiform Gyrus	139	3.6031	-18	6	-38

Supplementary Table 7. Clusters with significant correlations between activation and in-scanner semantic decision performance without controlling for lesion volume.

Sign	Peak Location	Extent	t-value	x	y	z
Positive	Cerebellar Vermis (VII)	9459	5.2166	-2	-78	-18
	L Angular Gyrus	9459	4.9495	-38	-72	48
	L Posterior Cingulate	9459	4.6985	-2	-32	32
	L Fusiform Gyrus	922	4.65	-32	-6	-38
	R Angular Gyrus	635	4.5575	54	-58	40
	L Middle Temporal Gyrus	1358	4.3664	-68	-32	-2
	L Inferior Temporal Gyrus	1358	3.7931	-50	-54	-22
	L Inferior Temporal Gyrus	1358	2.776	-40	-22	-10
	L Middle Orbital Gyrus	1000	4.3612	-42	54	0
	L Middle Orbital Gyrus	1000	2.8107	-24	30	-12
	L Parahippocampal Gyrus	706	4.3226	-22	-28	-18
	Dorsal Anterior Pons	678	4.1357	0	-12	-28
	R Inferior Temporal Gyrus	912	3.997	56	-12	-30
	R Temporal Pole	912	3.9832	36	14	-24
	R Cerebellum (III)	431	3.9087	20	-32	-22
	L Superior Frontal Gyrus	196	3.8601	-20	56	32
	R IFG (p. Orbitalis)	217	3.7043	50	38	-18
	L Rectal Gyrus	127	3.6622	2	24	-30
	L Superior Medial Gyrus	133	3.5319	2	54	42
	R Cerebellum (VIII)	154	3.1487	22	-54	-50
L Superior Medial Gyrus	147	3.0839	0	28	50	
Negative	L Superior Temporal Gyrus	346	-3.7382	-50	-8	6
	L Postcentral Gyrus	313	-3.6624	-56	-22	52
	R Posterior-Medial Frontal	160	-3.1177	2	4	68

Supplementary Table 8. Clusters with significant correlations between activation and fluency performance without controlling for lesion volume.

Sign	Peak Location	Extent	t-value	x	y	z
Positive	L Superior Medial Gyrus	29145	6.319	2	42	34
	L Fusiform Gyrus	29145	6.0604	-34	-18	-30
	L Middle Frontal Gyrus	29145	5.9276	-26	20	54
	R Fusiform Gyrus	2174	6.1538	36	-20	-36
	R Medial Temporal Pole	2174	4.8579	34	12	-30
	R Middle Temporal Gyrus	2174	4.8354	68	-16	-20
	R Angular Gyrus	261	5.2673	56	-60	42
Negative	L Superior Temporal Gyrus	247	-4.2095	-46	-14	2
	L Rectal Gyrus	171	-3.534	-8	30	-16

Supplementary Table 9. Clusters with significant correlations between activation and naming performance without controlling for lesion volume.

Sign	Peak Location	Extent	t-value	x	y	z
Positive	R Inferior Temporal Gyrus	1269	5.2377	46	2	-34
	R Fusiform Gyrus	1269	3.3062	16	4	-36
	R Superior Medial Gyrus	5123	5.0965	2	54	46
	L Middle Frontal Gyrus	5123	4.2917	-26	20	52
	L IFG (p. Triangularis)	5123	3.2481	-56	20	28
	R Cerebelum (IX)	1421	4.6445	12	-46	-38
	R Cerebelum (Crus II)	1421	3.2468	46	-56	-38
	L Middle Temporal Gyrus	5704	4.573	-46	-66	22
	L Posterior Cingulate	5704	4.0989	-2	-52	34
	R Precuneus	5704	3.7534	4	-56	66
	L Middle Temporal Gyrus	862	3.7835	-48	-36	-8
	L Precentral Gyrus	182	3.7823	-44	-6	30
	R Angular Gyrus	155	3.6659	56	-60	40
	L IFG (p. Orbitalis)	239	3.6576	-42	26	-16
	L Inferior Temporal Gyrus	277	3.4426	-54	-8	-30
	R Cerebelum (Crus 1)	217	3.4325	30	-80	-24
	Brainstem (Inf. Colliculus?)	131	3.1995	0	-28	-16
	Negative	L Superior Temporal Gyrus	215	-3.7198	-46	-18

Supplementary Table 10. Right hemispheric clusters with significant correlations between activation and lesion volume.

Sign	Peak Location	Extent	t-value	x	y	z
Positive	R IFG (p. Opercularis)	277	3.9446	56	12	8
	R Posterior-Medial Frontal	200	3.0469	8	6	56
	R Middle Frontal Gyrus	143	3.0383	34	40	20
	R Precentral Gyrus	221	2.9707	54	-2	40
Negative	R Inferior Temporal Gyrus	399	-4.1944	56	-14	-34
	R Mid Orbital Gyrus	223	-3.9815	2	46	4
	R Cerebellum (Crus I)	1137	-3.8737	56	-62	-32
	R Cerebellum (IX)	1137	-3.3749	14	-56	-48
	R Cerebellum (Crus I)	1137	-3.1767	34	-82	-24
	R Anterior Thalamus/Putami	160	-3.7215	10	-2	-6